Hybrid Energy Harvesting-Based Cooperative Spectrum Sensing and Access in Heterogeneous Cognitive Radio Networks

Abdulkadir Celik, *Member, IEEE,* Ahmad Alsharoa, *Student Member, IEEE,* and Ahmed E. Kamal, *Fellow, IEEE*

***Abstract*—In order to design energy efficient and energy harvesting (EEH) cooperative spectrum sensing (EEH-CSS), four fundamental constraints must be considered: 1) *collision constraint* to protect primary users (PUs) from the collision with secondary users (SUs), 2) *energy-causality constraint* which states that the energy harvested by a time instant must be greater than or equal to the consumed energy until that time instant, 3) *energy half-duplex* (EHD) constraint which prevents the batteries from charging and discharging at the same time, and 4) *correlation constraint* which limits the information about the primary channel (PC) state of next time slot can be extracted from the current PC state. In this regard, we consider a hybrid energy harvesting SU (EH-SU) model which can harvest energy from both renewable sources, e.g., solar, and ambient radio frequency signals. A heterogeneous EEH-CSS scheme is first proposed to handle EH-SUs with non-identical harvesting, sensing, and reporting characteristics by permitting them to sense and report at different sensing accuracy. Formulating the energy state evolution of EH-SUs with and without EHD constraint, we analyze the asymptotic activity behavior of a single EH-SU by deriving the theoretical upper bound for the chance of being active to sense and transmit. Thereafter, we develop a convex framework to find maximum achievable total throughput by optimizing the asymptotic active probability, sensing duration, and detection threshold of each SU subject to above constraints. Given a potential set of SUs, determining the optimal subset of cooperating EH-SUs is of the essence to achieve maximum achievable total throughput. Since EH-SU selection is inherently a combinatorial problem, a fast yet high performance solution is proposed based on SUs' energy harvesting, sensing and reporting attributes. Finally, a myopic access procedure is developed to determine the active set of EH-SUs given the best subset of SUs.**

***Index Terms*—Wireless Powered Communications, Myopic Policy, Poisson-Binomial, RF Energy Harvesting, Energy Half-Full Duplex, Correlation Constraint, Energy Causality Constraint.**

I. Introduction

To fulfill the ambitious demands of the next generation wireless communication networks, e.g., 1000 times the data traffic and 100^{th} of the energy consumption per bit [1], researchers in both academy and industry focus on *energy and spectrum efficient* solutions. CRNs have already received a great attention from both communities to mitigate the inefficient fixed spectrum allocation policy with the novel idea of utilizing idle licensed spectrum in an opportunistic and non-intrusive manner. However, a substantial portion of the above demands has recently migrated to mobile wireless networks and devices with limited energy resources. Considering the fact that 30% of the energy expenditure of mobile devices is caused by wireless networking and computing modules [2], energy efficient (EE) CRNs play a vital role to provide portable devices with more spectrum for less energy consumption. Because approximately 2% of the worldwide CO_2 emissions is caused by the communications and information technologies [3], EE policies are becoming more important to achieve green communication standards.

In this regard, recent studies focus on energy harvesting (EH) communications to obtain significant advantages over traditional grid-powered and non-rechargeable and/or battery-powered wireless devices. By harvesting required energy from alternative natural sources such as solar, vibrational, thermo-electric, and radio frequency (RF) signals etc., EH-SUs can achieve self-sustaining green communications. For a given amount of energy, conventional EE-CRNs aim to minimize the total sensing energy consumption subject to the fundamental *collision constraint* which prevents unlicensed users, i.e., SUs, from interfering with the licensed users, a.k.a primary users (PUs). In EH systems, on the other hand, energy needed for sensing and data transmission arrives intermittently and in random magnitudes of energy because of the random nature of EH sources. Then, the ultimate goal of EEH-CRNs would be, not only to minimize the over-all energy consumption, but to also maintain sensing and transmitting tasks under random and intermittent energy arrivals. Such a goal dictates an extra fundamental limit on the capacity of traditional CRNs: *energy-causality constraint* which states that the energy harvested by a time instant must be greater than or equal to the consumed energy until that time instant [4]. When the primary channel (PC) traffic is modeled as a Markov process, the information about the next spectrum occupancy state can be extracted from the current state is determined by the channel transition probabilities of the Markov process, which dictates *correlation constraint* as an additional design consideration [5].

A. Related Work

In his early work, Sultan considers a non-cooperative spectrum sensing scheme where a single EH-SU tries to maximize its throughput while making decision on being either dormant or active to sense the PC based on a Markov decision process (MDP) [6]. In [5], [7], [8], the authors investigate the effects of energy arrivals on spectrum sensing and access policies of

The authors are with the Department of Electrical and Computer Engineering, Iowa State University, Ames, IA 50011 USA (e-mail: akcelik@iastate.edu; alsharoa@iastate.edu; kamal@iastate.edu).

a single EH-SU. In accordance with the energy arrival rate, they also define *energy-limited* and *spectrum-limited* regimes for a fixed sensing duration. Nevertheless, these studies merely address the non-cooperative spectrum sensing. Moreover, they optimize the energy consumption of the SU by adjusting the detection threshold for a fixed sensing duration. However, joint optimization of sensing durations and detection thresholds of SUs is necessary for an EEH-CSS.

Yin et al. studies the fundamental tradeoffs among harvesting, sensing, and transmission duration in CSS [9]. Based on homogeneous signal-to-noise-ratio (SNR) and perfect common control channel (CCC) assumption, they develop the theoretical basis of CSS under the collision and EHD constraints. Likewise, for a homogeneous EH-CSS scenario where SUs harvest energy from RF signals, the optimal sensing probability and harvesting duration of each SU is obtained to maximize the throughput while satisfying the energy causality and PU collision constraints in [10]. Similarly, authors of [11] consider a homogeneous CSS setting to find the optimum balance between average probability of global detection, probability of false alarm and probability of having an active SU to transmit with the available harvested energy. Finally, a finite-horizon partially observable MDP (POMDP) is considered to obtain the optimal cooperation among the SUs for sensing and access to maximize throughput with the available energy while satisfying the collision constraint [12].

B. Main Contributions and Novelty

We summarize the main contributions of the paper as follows:

1) We first propose a *hybrid* EEH-CSS scheme of SUs which can harvest energy from renewable sources, e.g. solar, and ambient RF signals. This hybridization especially provides a general framework which is applicable to wireless and/or non-wireless EH-SUs with different size, power needs, and energy harvesting rate, etc. In order to mitigate the EHD limitation of ultra-capacitors, which prevents SUs from charging and discharging at the same time, Luo et al. proposed the simple and yet novel idea of using two different capacitors [13]. Based on our previous work [14], we also generalize their model to investigate the performance of a hybrid EEH-CSS with and without the EHD constraint.
2) Traditional K-out of-N rule treats SUs equivalently by enforcing each SU to report with identical local detector performances regardless of their sensing and reporting channel characteristics, which may not yield an optimal performance if SUs do not have identical sensing qualities. In order to obtain an optimal EEH-CSS scheme under heterogeneous conditions, we employ a heterogeneous K-out of-N rule by permitting SUs to report with different detector performance levels according to their sensing qualities. Demonstrating the differences in the time slotted operation of SUs due to the heterogeneity, we then develop the energy state evolution of EEH-CSS with and without EHD constraint.
3) Energy arrival rates, sensing durations and energy detection thresholds of EH-SUs are key factors in EEH-CSS since they are inextricably interwoven with the collision and energy-causality constraints. For the proposed hybrid model, we obtain the theoretical upper bound for the chance of being active subject to the energy causality and correlation constraints. Contingent upon the derived upper bound, we develop a convex framework to find maximum achievable total throughput by optimizing the active probability, sensing duration and detection threshold of each SU subject to the collision, energy causality, and correlation constraints.
4) Given a potential set of SUs, determining the optimal subset of cooperating SUs is of the essence to achieve maximum achievable total throughput. Selection of SUs inherently leads us into a combinatorial problem which has infeasible time complexity even for a moderate size of secondary networks (SNs) [15], [16]. Therefore, we propose a fast and high performance EH-SU selection heuristic based on SUs' energy harvesting, sensing and reporting attributes.
5) Optimal access policy of the EH-CRNs is typically formulated and studied using the POMDP framework. However, existing solution methods of POMDP are computationally intractable even for a single EH-SU because of continuous and uncountable state, action and observation spaces. Hence, we consider a myopic access policy by ignoring the effects of the current actions on the future rewards and focus only on the maximization of immediate reward of current time slot. In order to evaluate the performance of proposed methods under myopic access policy, we develop a *myopic access procedure* to determine the active set of EH-SUs since the energy cost of an EH-SU changes with different set of active EH-SUs.

The rest of this paper is organized as follows: Section II models the primary channel traffic and heterogeneous EEH-CSS model. Section III introduces the proposed hybrid EEH-CSS and energy state evolution of SUs. After that, Section IV analyzes the asymptotic behavior of the EEH-CSS and develop the proposed convex framework. Section V then explains the EH-SU selection heuristic and myopic access policy. Numerical results are presented in Section VI. Finally, we conclude the paper in Section VII with a few remarks. For their convenience, we refer interested readers to Table I for frequently used notations along with descriptions.

II. Heterogeneous EEH-CSS Model

We consider a single PC and an SN comprised of S self-powered EH-SUs each of which is synchronized with the primary network (PN) slot structure, and has different sensing, reporting, and energy harvesting characteristics. Denoting $\mathcal{M}$ by the set of M SUs chosen among S SUs to cooperatively sense the PC, Fig. 1 demonstrates a simple network scenario with $M = 5$ and $S = 10$. Our goal is to maximize achievable sum rate of the SN by selecting the optimal selection of M EH-SUs (i.e., EH-SU cluster) according to cooperative asymptotic behavior of the cluster which is mainly determined by cluster members' individual and distinctive sensing, harvesting, and reporting attributes. Given a cluster selection, it

Table of Notations	
Not.	**Description**
S	Total number of EH-SUs
M	Number of EH-SUs within the cluster, $1 \leq m \leq M$
T	Duration of a single time slot
H	Time horizon with indices, $1 \leq t \leq H$
$\mathcal{H}_0/\mathcal{H}_1$	Binary hypothesis for idle/busy PC state
$Z_m^{t,x}$	$Z_m^t = x$, $x \in \{0,1\}$
C_t	Actual PC occupancy state at time t: C_t^0 (idle), C_t^1 (busy)
p, q	State transition probabilities, i.e., p $(\mathcal{H}_0 \to \mathcal{H}_0)$, q $(\mathcal{H}_1 \to \mathcal{H}_1)$
π_0/π_1	Apriori prob. of being idle/busy
a_m^t	Mode indicator of SU m at time t: $a_m^{t,1}$ (active), $a_m^{t,0}$ (passive)
δ_m^t	Local decision of SU m at time t: $\delta_m^{t,0}$ $(\mathcal{H}_0)$, $\delta_m^{t,1}$ $(\mathcal{H}_1)$
ϕ_m^t	Global decision of the FC: ϕ_t^0 $(\mathcal{H}_0)$, ϕ_t^1 $(\mathcal{H}_1)$
θ_m^t	Acknowledgment for SU m at time t: $\theta_m^{t,0}$ (NACK), $\theta_m^{t,1}$ (ACK)
γ_m	Observed SNR by SU m on the PC
N_m	Number of samples taken by SU m
ε_m	Detection threshold of SU m
τ_m	Sensing duration of SU m
Γ_m	Sensing duration of the slowest SU, i.e., $\Gamma = \max_m(\tau_m)$
P_m^f/P_m^d	Local false alarm/detection probability of SU m
b_m^c	CCC error between SU m and the FC
$\bar{P}_m^f/\bar{P}_m^d$	Received false alarm/detection probability from SU m
$\mathcal{K}, \kappa$	Global test statistic $(\mathcal{K})$ and voting rule (κ)
Q_f/Q_d	Global false alarm/detection probability from SU m
$\chi_m^t/\chi_m^{t,RF}$	Renewable/RF energy arrival rate of SU m with mean χ_m/χ_m^{RF}
B_m	Battery capacity of SU m with state B_m^t at time t
R_m^t	Achievable throughput of SU m at time t
R_t	Total achievable throughput of SUs
E_m^s, E_m^{tx}	Sensing energy (E_m^s) and transmission energy (E_m^{tx}) of SU m
$E_m^{c,t}/E_m^{h,t}$	Consumed/Harvested energy by SU m at time t
α_m^0/α_m^1	Prob. of being active in idle/busy states s.t.
α_m	Prob. of being active for sensing and transmission.
$\bar{P}_m^f/\bar{P}_m^d$	Local prob. of being active and falsely/truly detecting the idle PC
$\bar{Q}_f/\bar{Q}_d$	Global prob. of being active and falsely/truly detecting the idle PC
$\bar{R}_m$	Asymptotically achievable throughput of SU m.
$\bar{R}$	Asymptotically achievable total throughput of SUs

Table I: Table of Notations

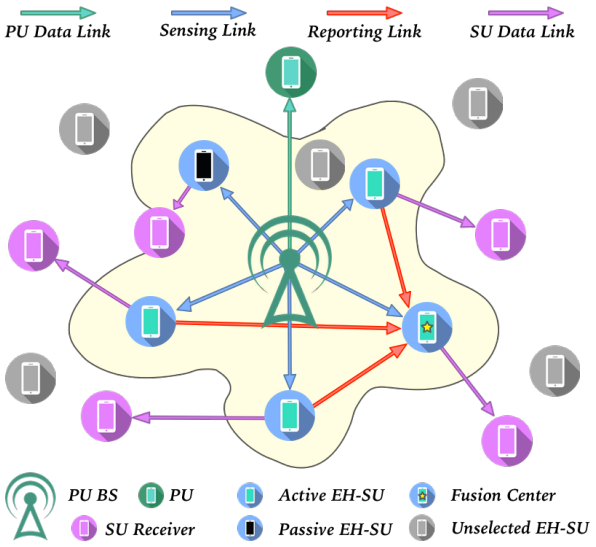

Fig. 1: Illustration of a time instant of the considered network model.

is also necessary to develop an access policy which decides on participation of SUs in sensing and channel utilization based on sensing outcome and EH-SUs' current battery level.

A. Primary Channel (PC) Traffic Model

We consider a PC with bandwidth W operating in a synchronous communication protocol with time-slots of duration T. We define a general notation Z_m^t where Z can be different variables with time index t and SU index m, if Z is a binary variable $Z_m^{t,x}$ means $Z_m^t = x$, $x \in \{0,1\}$. Likewise, Z_t^x simply means $Z_t = x$, $x \in \{0,1\}$. The PC occupancy state in slot t is denoted by $C_t \in \mathcal{C} \triangleq \{0(\mathcal{H}_0), 1(\mathcal{H}_1)\}$ where $\mathcal{H}_0$ and $\mathcal{H}_1$ represent the binary hypotheses for idle and busy PC states, respectively.

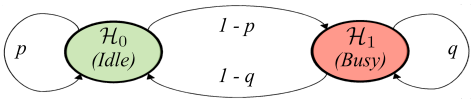

Fig. 2: Transition diagram of primary channel occupancy states.

Then, the PC traffic is modeled as a time-homogeneous discrete Markov process as shown in Fig. 2 where the PC stays in $\mathcal{H}_0$ $(\mathcal{H}_1)$ with probability p (q) and switches from $\mathcal{H}_0$ $(\mathcal{H}_1)$ to $\mathcal{H}_1$ $(\mathcal{H}_0)$ with probability $1-p$ $(1-q)$. Thus, state transition probabilities can be formulated as

$$\mathcal{P}\left[C_{t+1}^x | C_t\right] = \begin{cases} C_t(1-q) + (1-C_t)\ p & ,\ x = 0 \\ C_t\ q + (1-C_t)(1-p) & ,\ x = 1 \end{cases} \quad (1)$$

Assuming that the state transition probabilities are known to SUs via a long-term spectrum sensing history, the steady-state probabilities of being idle and occupied are given by $\pi_0 = \frac{1-q}{2-p-q}$ and $\pi_1 = \frac{1-p}{2-p-q}$, respectively. Please note that this model reduces to an *i.i.d.* random process with $\pi_0 = p$ and $\pi_1 = q$ if $p + q = 1$. Since SUs are merely interested in the PC channel activity, energy source of PUs (i.e., powered with/without energy harvesting) does not have any effect on the SN performance.

B. Heterogeneous Cooperative Spectrum Sensing Model

At the beginning of each slot, cooperating SUs first determine whether to be in the *active mode* to involve in CSS and data transmission or to be in the *passive mode* to solely harvest energy, which is denoted by $a_m^t \in A_m^t \triangleq \{0(passive), 1(active)\}$. If the passive mode is chosen, SU_m utilizes the whole slot for energy harvesting. Otherwise, SUs perform local spectrum sensing using energy detectors (EDs) which have been extensively exploited as the ubiquitous sensing technique in the literature due to their simplicity, compatibility with any signal type, and low computational and implementation complexity [17]. To detect primary signals, ED of SU_m measures the received primary signal energy for N_m number of samples and compares it with an energy threshold ε_m to make a local decision, $\delta_m^t \in \Delta_m^t \triangleq \{0(\mathcal{H}_0), 1(\mathcal{H}_1)\}$, on the PC state. For a sufficiently large N_m and normalized noise variance, the probability of false alarm, $P_m^f(N_m, \varepsilon_m) \triangleq$

$\mathcal{P}[\delta_m^{t,1}|a_m^{t,1},C_t^0]=\mathcal{P}[\delta_m^t=1|a_m^t=1,C_t=0]$, and the probability of detection, $P_m^d\left(N_m,\varepsilon_m,\gamma_m\right)\triangleq\mathcal{P}[\delta_m^{t,1}|a_m^{t,1},C_t^1]=\mathcal{P}[\delta_m^t=1|a_m^t=1,C_t=1]$, are respectively given by [18]

$$P_m^f=\mathcal{Q}\left[\left(\varepsilon_m-1\right)\sqrt{N_m}\ \right] \tag{2}$$

$$P_m^d=\mathcal{Q}\left[\left(\varepsilon_m-\gamma_m-1\right)\sqrt{\frac{N_m}{2\gamma_m+1}}\ \right] \tag{3}$$

where γ_m is the SNR of SU_m and $\mathcal{Q}\left(x\right)=\frac{1}{\sqrt{2\pi}}\int_x^{+\infty}e^{-y^2/2}dy$ is the right tail probability of a normalized Gaussian distribution. After the local sensing process, SUs report δ_m^t to a fusion center (FC) over a binary symmetric CCC. Denoting the received local decision by the FC as $\tilde{\delta}_m^t\in\tilde{\Delta}_m^t$, received P_m^f and P_m^d at the FC side are given by

$$\tilde{P}_m^f=b_m^c\left(1-P_m^f\right)+\left(1-b_m^c\right)P_m^f \tag{4}$$

$$\tilde{P}_m^d=b_m^c\left(1-P_m^d\right)+\left(1-b_m^c\right)P_m^d \tag{5}$$

where $b_m^c=\mathcal{P}[\tilde{\delta}_m^t=1|\delta_m^t=0]=\mathcal{P}[\tilde{\delta}_m^t=0|\delta_m^t=1]$ is the bit error rate of the symmetric CCC between SU_m and the FC. The FC collects $\tilde{\delta}_m^t$ from all SUs in the cluster and makes a global decision, $\varphi_t\in\Phi_t\triangleq\{0(\mathcal{H}_0),1(\mathcal{H}_1)\}$, using the following test

$$\mathcal{K}=\sum_{m=1}^{M}\tilde{\delta}_m^t\underset{\varphi_t^0}{\overset{\varphi_t^1}{\gtrless}}\kappa \tag{6}$$

which is summation of the independent but non-identically distributed *Bernoulli* random variables, thus, follows the *Poisson-Binomial distribution*. Based on (2)-(6), the FC obtains the global false alarm, $Q_f\triangleq\mathcal{P}[\mathcal{K}\geq\kappa|\mathcal{H}_0]=\mathcal{P}\left[\varphi_t^1|C_t^0\right]$, and global detection probability, $Q_d\triangleq\mathcal{P}[\mathcal{K}\geq\kappa|\mathcal{H}_1]=\mathcal{P}\left[\varphi_t^1|C_t^1\right]$, by fusing the local reports as follows [19]

$$Q_f(\tilde{P}_m^f)=\sum_{i=\kappa}^{M}\sum_{A\in F_i}\prod_{m\in A}\tilde{P}_m^f\prod_{m\in A^c}\left(1-\tilde{P}_m^f\right) \tag{7}$$

$$Q_d(\tilde{P}_m^d)=\sum_{i=\kappa}^{M}\sum_{A\in F_i}\prod_{m\in A}\tilde{P}_m^d\prod_{m\in A^c}\left(1-\tilde{P}_m^d\right) \tag{8}$$

where F_i is the set of all subsets of i integers that can be selected from $\{1,2,3,\ldots,M\}$. Q_f and Q_d can be expeditiously calculated from polynomial coefficients of the probability generating function of $\mathcal{K}$ in $O(M\log M)$ [20]. At the end of each slot, the secondary receiver acknowledges a successful transmission, expressed here as $\theta_m^t\in\Theta_m^t\triangleq\{0(\text{NACK}),1(\text{ACK})\}$.

III. Hybrid Energy Harvesting and Energy State Evolution of EH-SUs

A. Hybrid Energy Harvesting

We consider EH-SUs with the ability of harvesting energy from renewable sources (e.g. solar) and ambient RF/wireless signals (e.g., primary signals). Simultaneous wireless information and power transfer technique has been recently proposed where the receiver is able to use the radio frequency signal simultaneously for information and energy harvesting [21]. On the other hand, two main practical protocols are proposed in the literature namely; time switching (TS) protocol and power splitting (PS) protocol. In the TS protocol, the energy harvesting node switches over time between the energy harvester equipment and the information decoder, while in PS protocol, a portion of the received signal is used for energy harvesting and the remaining is used for the information processing [22]. In this paper, we focus on the TS protocol such that time is split for harvesting, sensing, and transmission tasks. We define composite stochastic energy arrival rate from renewable/RF energy source of SU_m within a slot t as the product of amount of received energy per time unit, i.e., $[Joules/s]$, battery efficiency, and energy harvester efficiency. While renewable composite energy arrival at time t is denoted as χ_m^t, which is modeled as a Gamma random variable with mean χ_m, composite RF energy arrival rate of slot t is denoted as $\chi_m^{t,RF}$, which is similarly modeled as a Gamma random variable with the mean value of χ_m^{RF} [14]. For example, χ_m^t can be interpreted as the net accumulated energy per time unit with respect to received luminous intensity of a solar panel in a particular direction per unit solid angle. When both energy sources are simultaneously utilized, total composite energy arrival rate is the summation of energy arrivals from both sources, i.e., $\chi_m^t+\chi_m^{t,RF}$ with mean $\chi_m+\chi_m^{RF}$. We assume that χ_m^t and $\chi_m^{t,RF}$ are time invariant during a slot duration. SU_m first buffers the harvested energy, then stores it in a battery with capacity B_m. While the energy arrival information is causally available to the SU_m, residual energy from slot t, B_m^t, is available at the beginning of slot $t+1$.

To store harvested energy, ultra-capacitors, a.k.a super-capacitors, are mostly preferred due to their high power density, good recycling ability, and near perfect storing efficiency. Albeit these favorable features, ultra-capacitors are subject to the *energy half-duplex* (EHD) constraint which prevents SUs from charging and discharging simultaneously [13]. This constraint can be mitigated by the exploitation of two identical ultra-capacitors such that while the first one charges from harvested energy, the second discharges to supply continuous power for sensing and transmission tasks [13], [14]. Thus, we consider two different EEH-CSS schemes with and without the EHD constraint and refer to them as energy half-duplex systems (EHS) and energy full-duplex systems (EFS), respectively. Time slotted operation of active EH-SUs ($a_1^t=a_m^t=a_M^t=1$) with heterogeneous SNRs ($\gamma_1<\gamma_m<\gamma_M$) and reporting errors ($b_M^c<b_m^c<b_1^c$) are illustrated in Fig. 3 where T_s, $\tau_m=N_mT_s$, and $\Gamma=\max_m\left(\tau_m\right)$ represent the sample duration, sensing duration of SU_m, and sensing duration of the slowest SU which is defined as the SU with the longest sensing duration, respectively.

In the EHS, active SUs first execute local spectrum sensing, then they harvest and store renewable energy until the global decision is received. On the contrary, SUs are capable of harvesting the renewable energy for the entire slot in the EFS where SUs go into sleep until the global decision feedback when they do not sense. During the sleep, consumed energy and the leakage from the battery is assumed to be negligible. After the slowest SU reports its local decision, the FC makes

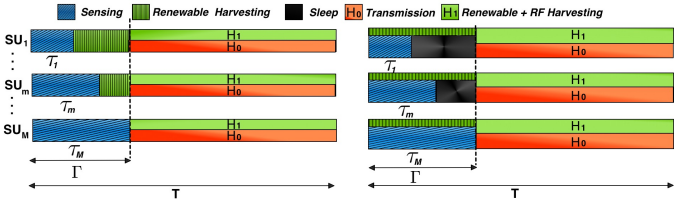

(a) EHS with Energy Half-Duplex Constraint (b) EFS without Energy Half-Duplex Constraint

Fig. 3: TS protocol and timeslot illustration of active EH-SUs, i.e. $a_1^t = a_m^t = a_M^t = 1$, with heterogeneous SNRs and reporting errors.

a global decision based on which the remaining time is used for transmission (φ_t^0) or RF-EH (φ_t^1). As a result, the EHD constraint intuitively causes a performance degradation in the amount of harvested energy because SUs have to share the available time for harvesting, sensing, and transmitting.

B. Energy State Evolution of SUs

In EEH-CSS, energy states of SUs evolve over time such that energy state in the next timeslot depends on the energy state (B_m^t), actions (a_m^t) and decisions ($\delta_m^t, \tilde{\delta}_m^t, \varphi_t$) taken in the current timeslot. Based on Fig. 3, energy consumption of SU_m in slot t can be expressed as

$$E_m^{c,t} = a_m^t \left[E_m^s + \varphi_t E_m^{tx}\right] \tag{9}$$

where $E_m^s = P_m^s \tau_m$ is the sensing energy, P_m^s is the sensing power, and E_m^{tx} is the energy consumption within a transmission phase which is modeled as

$$E_m^{tx} = \left(P_m^c + \frac{\xi_m}{\zeta_m} P_m^t\right)(T - \Gamma) \tag{10}$$

where P_m^t is the transmission power, ζ_m is the drain efficiency of the power amplifier (PA), ξ_m is the peak-to-average ratio (PAR) of PA, and P_m^c is the power consumed in various transmitter and receiver circuitry except the PA power [23]. Based on the discussion in previous subsection and Fig. 3, amount of harvested energy in EHS on slot t can be given as

$$E_m^{h,t} = \begin{cases} (1 - a_m^t)\,\chi_m^t T & , a_m^{t,0}, C_t, \varphi_t \text{ for EHS} \\ a_m^t \chi_m^t\,(\Gamma - \tau_m) & , a_m^{t,1}, C_t, \varphi_t \text{ for EHS} \\ a_m^t \varphi_t \chi_m^t\,(T - \Gamma) & , a_m^{t,1}, C_t, \varphi_t^1 \text{ for EHS} \\ a_m^t C_t \varphi_t \chi_m^{t,RF}\,(\Gamma - \tau_m) & , a_m^{t,1}, C_t^1, \varphi_t^1 \text{ for EHS} \\ 0 & , \text{otherwise} \end{cases} \tag{11}$$

where we have the following EH event types: 1) $a_m^{t,0}, C_t, \varphi_t$: Passive mode is chosen. Regardless of C_t and φ_t, entire timeslot is used for renewable EH, 2) $a_m^{t,1}, C_t, \varphi_t$: Active mode is chosen and CSS is being performed. Regardless of C_t and φ_t, the SU performs renewable EH until the slowest SU completes sensing task, 3) $a_m^{t,1}, C_t, \varphi_t^1$: Active mode is chosen and CSS is performed. The PC is globally decided to be idle, thus, SUs do not transmit but perform renewable EH until the end of slot, and 4) $a_m^{t,1}, C_t^1, \varphi_t^1$: Active mode is chosen and CSS is performed. The PC is globally decided to be busy while it is indeed busy. Thus, SUs harvest RF energy from ongoing PU activity. Equation (11) can easily be adopted for EFS which can harvest the renewable energy all the time while it can only perform RF-EH in event type 4 as in EHS. All of these cases can be put in a compact form as shown in (12). Exploiting (9) and (12), available residual energy level at the beginning of the slot $t+1$ is given by

$$B_m^{t+1} = \min\left(B_m, B_m^t + E_m^{h,t} - E_m^{c,t}\right) \tag{13}$$

Assuming that the secondary transmission is successful if and only if the PC is in idle state and secondary transmitters receive an acknowledgement from the secondary receivers, the total achievable throughput of the SN is given by

$$R_t = \begin{cases} \pi_0(1 - Q_f) \sum_m R_m^t & , \text{if } C_t^0, a_m^{t,1}, \varphi_t^0, \theta_m^{t,1} \\ 0 & , \text{otherwise} \end{cases} \tag{14}$$

where $R_m^t = \frac{T-\Gamma}{T} \log_2\left[1 + \frac{P_m^t h_m^t}{N_0 W}\right]$ is the achievable throughput of SU_m, h_m^t is the channel gain between SU_m and its receiver, and N_0 is the noise power spectral density of the receiver.

IV. Asymptotic Analysis of Energy Harvesting Cooperative Spectrum Sensing (EEH-CSS)

Sensing duration is a major sensing parameter since it is inextricably interwoven with the collision and energy-causality constraints. Although sensing for a longer duration yields more protection from collision with PUs, it results in extra sensing energy cost, fewer harvested energy, and reduced achievable throughput due to the less time left for secondary transmission. Therefore, the sensing duration establishes the fundamental tradeoff between these two major constraints. In other words, sensing longer grants less collision probability in return for fewer chance to be in the active mode due to the reduced energy availability. Detection threshold is another key sensing parameter such that setting a higher threshold yields more collision probability and less chance to utilize the idle PC states. Therefore, optimization of sensing duration and detection threshold is a necessity to obtain an optimal performance. Under the cooperation of EH-SUs, on the other side, determination of an optimal framework typically necessitates a much more involved design since we are also required to find an optimal tradeoff among cooperating SUs with respect to their sensing, reporting and energy harvesting characteristics.

For given feasible sensing durations and detection thresholds of cooperating SUs, we first consider asymptotic activity pattern of a single SU over an infinite time-horizon and infinite battery capacity such that the average energy causality constraint dictates the average amount of harvested energy not to be less than the average amount of consumed energy [7]. Since we consider the average values over an infinite time-horizon, we omit the superscript t throughout this section. Denoting the probability of being active in idle and busy PC state as $\alpha_m^0 \triangleq \mathcal{P}\left[a_m^1 | \mathcal{H}_0\right]$ and $\alpha_m^1 \triangleq \mathcal{P}\left[a_m^1 | \mathcal{H}_1\right]$, respectively, probability of being active to sense and transmit (if the PC is found idle) for SU_m can be given by

$$\alpha_m = \pi_0 \alpha_m^0 + \pi_1 \alpha_m^1 \tag{15}$$

which is an essential metric reflecting the cooperation chance of SU_m based on its sensing/reporting quality, energy consumption and arrival properties. As per (15), local probability

$$E_m^{h,t} = \begin{cases} \underbrace{\left(1-a_m^t\right)\chi_m^t T}_{\text{EH Event Type 1}} + a_m^t \left\{ \underbrace{\chi_m^t\left(\Gamma-\tau_m\right)}_{\text{EH Event Type 2}} + \underbrace{\varphi_t \chi_m^t \left(T-\Gamma\right)}_{\text{EH Event Type 3}} + \underbrace{C_t \varphi_t \chi_m^{t,RF}\left(T-\Gamma\right)}_{\text{EH Event Type 4}} \right\} & \text{, EHS} \\ \underbrace{\chi_m^t T}_{\text{Always}} + \underbrace{a_m^t C_t \varphi_t \chi_m^{t,RF}\left(T-\Gamma\right)}_{\text{EH Event Type 4}} & \text{, EFS} \end{cases} \tag{12}$$

of being active and falsely deciding the idle PC as busy, $\bar{P}_m^f \triangleq \mathcal{P}\left[\delta_m^1, a_m^1 | \mathcal{H}_0\right]$, and local probability of being active and truly deciding the busy PC as busy, $\bar{P}_m^d \triangleq \mathcal{P}\left[\delta_m^1, a_m^1 | \mathcal{H}_1\right]$, are given by

$$\bar{P}_m^f = \alpha_m^0 P_m^f \leq P_m^f \tag{16}$$
$$\bar{P}_m^d = \alpha_m^1 P_m^d \leq P_m^d \tag{17}$$

where P_m^f and P_m^d are energy unconstrained false alarm and detection probabilities where SUs can always be active to sense and transmit (i.e., $\alpha_m = \alpha_m^0 = \alpha_m^1 = 1$), respectively. Then, substituting $\bar{P}_m^f$ and $\bar{P}_m^d$ into (4) and (5), $\bar{Q}_f$ and $\bar{Q}_d$ can be obtained from (7) and (8), respectively. Therefore, the expected energy consumption can be derived from (9) as

$$E_m^c = \alpha_m^0 E_m^{c,0} + \alpha_m^1 E_m^{c,1} \tag{18}$$
$$E_m^{c,0} = \pi_0 \left[E_m^s + \left(1-\bar{Q}_f\right) E_m^{tx}\right] \tag{19}$$
$$E_m^{c,1} = \pi_1 \left[E_m^s + \left(1-\bar{Q}_d\right) E_m^{tx}\right] \tag{20}$$

where (19) and (20) denote the expected energy cost within the idle and busy PC states, respectively. Probabilities for the energy harvesting event types given in Section III-B can be given as follows

1) $\mathcal{P}\left[E_m^{h,t} | a_m^{t,0}, C_t, \varphi_t\right] = 1-\alpha_m = 1-\pi_0\alpha_m^0 - \pi_1\alpha_m^1$
2) $\mathcal{P}\left[E_m^{h,t} | a_m^{t,1}, C_t, \varphi_t\right] = \alpha_m = \pi_0\alpha_m^0 + \pi_1\alpha_m^1$
3) $\mathcal{P}\left[E_m^{h,t} | a_m^{t,1}, C_t, \varphi_t^1\right] = \pi_0\alpha_m^0\bar{Q}_f + \pi_1\alpha_m^1\bar{Q}_d$
4) $\mathcal{P}\left[E_m^{h,t} | a_m^{t,1}, C_t^1, \varphi_t^1\right] = \pi_1\alpha_m^1\bar{Q}_d$

Accordingly, the expected amount of harvested energy in EHS is derived from (12) as follows

$$\begin{aligned} E_m^h &\triangleq \mathbb{E}\left[E_m^{h,t}\right]_t = (1-\pi_0\alpha_m^0 - \pi_1\alpha_m^1)\chi_m T \\ &+ (\pi_0\alpha_m^0 + \pi_1\alpha_m^1)\chi_m(\Gamma-\tau_m) \\ &+ [\pi_0\alpha_m^0\bar{Q}_f + \pi_1\alpha_m^1\bar{Q}_d]\chi_m(T-\Gamma) + \pi_1\alpha_m^1\bar{Q}_d\chi_m^{RF}(T-\Gamma) \\ &= \chi_m T + \alpha_m^0 A_m + \alpha_m^1(B_m+C_m) \end{aligned} \tag{21}$$
$$A_m = \pi_0\chi_m\left[\left(\bar{Q}_f - 1\right)(T-\Gamma) - \tau_m\right] \tag{22}$$
$$B_m = \pi_1\left[\chi_m\{(\bar{Q}_d-1)(T-\Gamma)-\tau_m\} + \chi_m^{RF}\bar{Q}_d(T-\Gamma)\right]$$
$$C_m = \pi_1\bar{Q}_d\chi_m^{RF}(T-\Gamma) \tag{23}$$

which can easily be adopted for EFS by setting $A_m = 0$ and replacing B_m with C_m. Then, *the expected energy causality constraint*, $E_m^c \leq E_m^h$, can be derived from (18)-(23) as

$$\alpha_m^0(E_m^{c,0} - A_m) + \alpha_m^1(E_m^{c,1} - B_m) \leq \chi_m T, \text{ for EHS} \tag{24}$$
$$\alpha_m^0 E_m^{c,0} + \alpha_m^1(E_m^{c,1} - C_m) \leq \chi_m T, \text{ for EFS} \tag{25}$$

Since p and q quantify the amount of information about C_{t+1} that can be extracted from C_t, considered Markovian PC traffic model mandates the following *correlation constraint*

$$\ell \leq \alpha_m^1/\alpha_m^0 \leq \upsilon \tag{26}$$

where $\ell = \max\left[\frac{1-\max(p,1-q)}{\max(p,1-q)}, \frac{\min(1-p,q)}{1-\min(1-p,q)}\right]\frac{1-q}{1-p}$ and $\upsilon = \min\left[\frac{1-\min(p,1-q)}{\min(p,1-q)}, \frac{\max(1-p,q)}{1-\max(1-p,q)}\right]\frac{1-q}{1-p}$ [8].

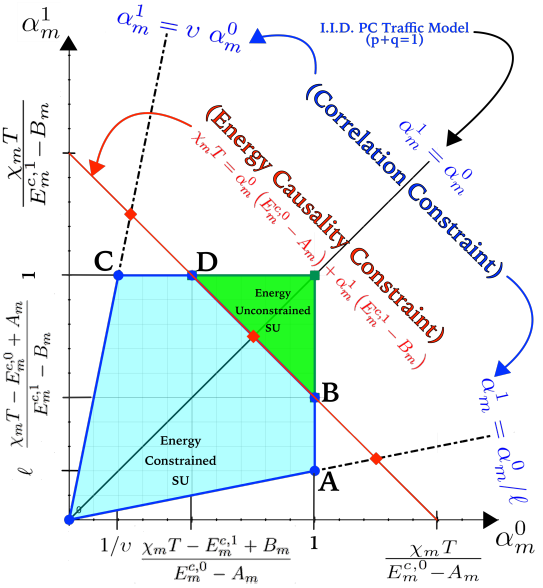

Fig. 4: Feasible region of α_m^0 and α_m^1 in EHS for a given (N_m, ε_m).

The energy causality constraint in (24) and the correlation constraint in (26) is visualized in Fig. 4 which demonstrates the feasible region of the EHS for a given (N_m, ε_m). The energy causality constraint is shown as a solid-red line which forms the energy constrained and energy unconstrained EHS as polygonal convex regions in checkered-cyan and solid-green colors, respectively. Energy constrained (unconstrained) SUs can be defined as SUs whose average harvested energy is less (equal or higher) than the average energy consumption. On the other hand, the dashed-black lines illustrate the correlation constraint which determines the relation between α_m^0 and α_m^1 as a function of channel transition probabilities p and q. Physical interpretation of correlation constraint can be inferred from its effect on the feasible region which reduces to solid-black line ($\alpha_m^0 = \alpha_m^1$) in Fig. 4 if the PC traffic as an i.i.d. random process. Accordingly, energy causality and correlation constraints is projected on the asymptotic upper bound of α_m^0 and α_m^1 as in Theorem 1.

Theorem 1: *Assuming an infinite time-horizon and $B_m \to \infty$, the upper bounds on probability of being active in idle and busy states under the energy causality and correlation*

constraints are found for the EHS as

$$\bar{\alpha}_m^0(N_m,\varepsilon_m,\chi_m)=\min\left(1,\frac{\chi_m T}{E_m^{c,0}-A_m+\ell(E_m^{c,1}-B_m)}\right) \quad (27)$$

$$\bar{\alpha}_m^1(N_m,\varepsilon_m,\chi_m)=\min\left(1,\frac{\upsilon\chi_m T}{E_m^{c,0}-A_m+\upsilon(E_m^{c,1}-B_m)}\right) \quad (28)$$

Upper bounds for EFS can be obtained from (27) and (28) by setting $A_m=0$ and replacing B_m with C_m.
Proof: *Please see Appendix A.*

Corollary 1: *Upper bound on sensing probability is given by*

$$\bar{\alpha}_m=\pi_0\bar{\alpha}_m^0+\pi_1\bar{\alpha}_m^1 \quad (29)$$

Proof: *This corollary is an immediate result of (15) and Theorem 1.*

In what follows, $\mathbf{P}_1$ formulates the optimal EEH-CSS which maximizes the total achievable throughput of the secondary network subject to the collision, energy causality, and correlation constraints.

$$\begin{aligned}
\mathbf{P_1}: &\underset{\substack{\alpha_m^0,\alpha_m^1\\ N_m,\varepsilon_m,\,\forall m}}{\text{maximize}} && \bar{R}=\pi_0(1-\bar{Q}_f)\sum_m R_m\\
\text{C1:}\quad &\text{s.t.} && Q_d^{th}\le\bar{Q}_d\\
\text{C2:}\quad & && \bar{Q}_f\le Q_f^{th}\\
\text{C3:}\quad & && 0\le\alpha_m^0\le\bar{\alpha}_m^0,\ \forall m\\
\text{C4:}\quad & && 0\le\alpha_m^1\le\bar{\alpha}_m^1,\ \forall m\\
\text{C5:}\quad & && 30\le N_m\le T/T_s,\ \forall m\\
\text{C6:}\quad & && N_m\in\mathbb{R}^+,\ \varepsilon\in\mathbb{R},\ \forall m
\end{aligned}$$

Constraints C1 and C2 satisfy the collision and spectrum utilization constraint by ensuring Q_d^{th} and Q_f^{th} global detection and false alarm probabilities, respectively. C3 and C4 assure the energy causality and correlation constraints according to Theorem 1. N_m is lower-bounded to evoke the central limit theorem and is upper-bounded by the maximum permissible number of samples within a slot duration in C5. The domains of variables are indicated in C6. $\mathbf{P_1}$ is a mixed integer nonlinear programming problem due to the integer valued number of samples. A practical approach to relax $\mathbf{P_1}$ is unintegerization of N_m, which does not violate the the problem constraints or negatively effect the system performance since $N_m >> 1$ and $T_s << 1$ in general.

However, unintegerized $\mathbf{P_1}$ is still not jointly convex in $(N_m,\varepsilon_m,\alpha_m^0,\alpha_m^1)$, $\forall m$. To alleviate this issue, we transform $\mathbf{P_1}$ into a convex *bilevel optimization problem* with a convex upper level problem, $\mathbf{P_1^u}$, and a convex lower level problem, $\mathbf{P_1^l}$. In an iterative manner and subject to common constraints C1-C7, while $\mathbf{P_1^u}$ maximizes $\log(\bar{R})$ for a given $N_m,\forall m$ obtained from $\mathbf{P_1^l}$, $\mathbf{P_1^l}$ maximizes $\log(\bar{R})$ for a given $(\varepsilon,\alpha_m^0,\alpha_m^1)$, $\forall m$, obtained from $\mathbf{P_1^u}$. In the considered bilevel problem, we take the logarithm of $\bar{R}$, $\bar{Q}_f$, and $\bar{Q}_d$ in order to put them into convex form by exploiting the convex composition rules, log-concavity of Poisson-Binomial distribution, convexity of q-functions for $P_m^f=\mathcal{Q}(\cdot)\le 0.5$, and concavity of q-functions for $P_m^d=\mathcal{Q}(\cdot)\ge 0.5$. Please note that $P_m^f\le 0.5$ and $P_m^d\ge 0.5$ do not conflict with the practical point of interest and can be satisfied by introducing an additional constraint on detection threshold as in C5. We refer interested readers to Appendix B and references therein for a formal convexity analysis of $\mathbf{P_1^u}$ and $\mathbf{P_1^l}$.

$$\begin{aligned}
\mathbf{P_1^u}: &\underset{\substack{\alpha_m^0,\alpha_m^1\\ \varepsilon_m,\,\forall m}}{\text{maximize}} && \log\left(\bar{R}\right)\\
\mathbf{P_1^l}: &\underset{N_m,\,\forall m}{\text{maximize}} && \log\left(\bar{R}\right)\\
\text{C1:}\quad &\text{s.t.} && \log(Q_d^{th})\le\log(\bar{Q}_d)\\
\text{C2:}\quad & && \log(\bar{Q}_f)\le\log(Q_f^{th})\\
\text{C3:}\quad & && 0\le\alpha_m^0\le\bar{\alpha}_m^0,\ \forall m\\
\text{C4:}\quad & && 0\le\alpha_m^1\le\bar{\alpha}_m^1,\ \forall m\\
\text{C5:}\quad & && 1\le\varepsilon\le 1+\gamma_m,\ \forall m\\
\text{C6:}\quad & && 30\le N_m\le T/T_s,\ \forall m\\
\text{C7:}\quad & && N_m\in\mathbb{R}^+,\ \varepsilon\in\mathbb{R},\ \forall m
\end{aligned}$$

V. SU Selection and Spectrum Access Policy

A. EH-SU Selection Heuristic

In previous sections, EEH-CSS is investigated for a given set of SUs, $\mathcal{M}$. However, determining the optimal $\mathcal{M}$ is of the essence to achieve a desirable achievable total throughput. To illustrate, selection of an SU with insufficient energy arrival rate may not often be available to cooperate due to the energy causality constraint, which inherently degrades the group performance. Even if an SU has a profitable energy arrival rate, sensing quality (i.e. SNR) is another key factor to count in for energy causality and sensing duration. For instance, an SU with high energy arrival rate and low SNR can always be active to cooperate. Nevertheless, its low SNR may require very long sensing duration which reduces the transmission time and throughput of the entire group. Furthermore, CCC imperfection is another crucial practical issue since an SU must compensate the reporting error by executing more accurate local sensing which yields less time for transmission, more energy cost, and thus fewer availability to cooperate. Please also note that after a certain error rate, which is also known as *bit error probability (BEP) wall* [15], [24], there is no feasible cooperation no matter how much time and energy are spent for sensing. Determination of the optimal $\mathcal{M}$ leads to a combinatorial problem which requires impractically high computational complexity.

Therefore, we propose a fast and high performance EH-SU selection heuristic in Algorithm 1 to determine the best $\mathcal{M}$. In Algorithm 1, lines 1-3 first evaluate the individual (non-cooperative) asymptotic sensing performance of SUs, $\bar{R}_j$, then it ranks the SUs in the descending order of $\bar{R}_j$ in line 4. After the initialization step in line 5, the while loop forms the best $\mathcal{M}$ starting from the SU with the highest rank, which is terminated with the SU that deteriorates the total achievable throughput, i.e., $\Delta<0$. Such a situation occurs when acceptance SU_i to the cluster reduces the transmission time of current cluster members (SU_1-SU_{i-1}) and data rate of SU_i cannot compensate the data rate loss of current members, i.e., cluster sum rate is reduced by accepting SU_i. While the *for* and *while* loops take $O(S)$ steps, sorting operation in line 4 is $O(S\log S)$. Thus, the overall complexity of Algorithm 1 is $O(S\log S)$.

Algorithm 1 EH-SU Selection Heuristic

Input: χ_m, γ_m, b_m^c, $\forall m$
Output: The best total throughput and corresponding SU set.
1: **for** $j = 1$ to S **do**
2: Compute $\bar{R}_j = \pi_0(1 - \bar{Q}_f)R_j$ using $\mathbf{P_1^l}$ and $\mathbf{P_1^u}$
3: **end for**
4: $\boldsymbol{O} \leftarrow$ Sort SUs in descending order wrt $\bar{R}_j$.
5: $\bar{R}_0 \leftarrow 0$, $\Delta \leftarrow 0$, $i \leftarrow 1$, $\mathcal{M} \leftarrow \emptyset$, $\mathcal{M}^\star \leftarrow \emptyset$, $R^\star \leftarrow 0$
6: **while** $\Delta \geq 0$ && $i \leq S$ **do**
7: $\mathcal{M} \leftarrow SU_i$ Accept the SU ranked i^{th} in $\boldsymbol{O}$.
8: $\bar{R}_i \leftarrow$ Compute $\bar{R}$ for $\mathcal{M}$ using $\mathbf{P_1^l}$ and $\mathbf{P_1^u}$
9: $\Delta \leftarrow \bar{R}_i - \bar{R}_{i-1}$
10: **if** $\Delta \geq 0$ **then**
11: $R^\star \leftarrow \bar{R}_i$
12: $\mathcal{M}^\star \leftarrow \mathcal{M}$
13: **end if**
14: $i \leftarrow i + 1$
15: **end while**
16: **return** $R^\star$, $\mathcal{M}^\star$

B. Spectrum Access Policy

Optimal spectrum access policy of EH-CRNs is typically studied in the realm of POMDP which can be defined as a tuple $(\mathcal{S}, \mathcal{A}, \mathcal{O}, \mathcal{R}) = \{(\mathcal{S}_t, \mathcal{A}_t, \mathcal{O}_t, \mathcal{R}_t)\,|\forall t\}$, where

- $\mathcal{S}_t \triangleq \mathcal{C}_t \times B_t$ is the global state space consisting of battery level of SUs, $B_t = \{B_m^t|\forall m\}$, and PC occupancy state.
- $\mathcal{A}_t \triangleq A_t \times \Delta_t$ is the global action space where $A_t = \{A_m^t|\forall m)\}$ and $\Delta_t = \{\Delta_m^t|\forall m\}$.
- $\mathcal{O}_t \triangleq \tilde{\Delta}_t \times \Phi_t \times \Theta_t$ is the global observation space where $\tilde{\Delta}_t = \{\tilde{\Delta}_m^t|\forall m\}$ and $\Theta_t = \{\Theta_m^t|\forall m\}$.
- $\mathcal{R}_t \triangleq \{R_m^t|\forall m\}$ is the global reward space.

Since $(\mathcal{S}, \mathcal{A}, \mathcal{O}, \mathcal{R})$ is continuous and uncountable, it can be found that existing solution methods for optimal access policy are computationally intractable, and cannot be employed in practice even for a single SU [9]. In EEH-CSS, complexity and communication overhead exponentially grow with the increasing number of cooperating SUs. Without recourse to optimal POMDP solution, we then focus on the *myopic policy optimization* by ignoring the effects of the current actions on the future rewards and consider only maximization of the immediate reward of current time slot. Existing studies have shown that myopic access policy has a close performance to the optimal policy with a significantly reduced computational complexity [25], [26]. Regardless of the underlying PC state, the immediate reward of an SU operating on myopic access policy can be maximized by involving in cooperation whenever there is sufficient energy to execute sensing and transmission. In this case, SUs greedily decide on the participation in sensing based on the following action policy

$$a_m^t = \begin{cases} 1 & , \; B_m^t \geq E_m^{th} \\ 0 & , \; B_m^t < E_m^{th} \end{cases}, \forall m \tag{30}$$

where $E_m^{th} = E_m^s + [\pi_0(1 - Q_f^{th}) + \pi_1(1 - Q_d^{th})]E_m^{tx}$ is a function of N_m which is jointly determined by other active SUs, $a_{m'}^t, \forall m' \neq m$. Therefore, an evaluation procedure for (30) is necessary to jointly determine active SUs within a slot.

Based on average SNR values, we first create an offline table for $\boldsymbol{E} \in \mathbb{R}^{|\mathcal{M}^\star| \times 2^{|\mathcal{M}^\star|}}$ where columns represent $2^{|\mathcal{M}^\star|}$ permutations, which takes $\mathcal{O}\left(2^{|\mathcal{M}^\star|}\right)$. For the heterogeneous case, N_m can be determined similar to $\mathbf{P}_1^u$ and $\mathbf{P}_1^l$ as follows

$$\begin{aligned}
\mathbf{P_2^u}: & \underset{\varepsilon_m,\, \forall m}{\text{maximize}} && \log\left(R_t\right) \\
\mathbf{P_2^l}: & \underset{N_m,\, \forall m}{\text{maximize}} && \log\left(R_t\right) \\
\text{C1:} & \text{s.t.} && \log(Q_d^{th}) \leq \log(Q_d) \\
\text{C2:} & && \log(Q_f) \leq \log(Q_f^{th}) \\
\text{C3:} & && 1 \leq \varepsilon \leq 1 + \gamma_m, \; \forall m \\
\text{C4:} & && 30 \leq N_m \leq T/T_s, \; \forall m \\
\text{C5:} & && N_m \in \mathbb{R}^+, \; \varepsilon \in \mathbb{R}, \; \forall m
\end{aligned}$$

Under the traditional approach, SUs are required to ensure that the FC receives identical local false alarm and detection probability reports, i.e. $\tilde{P}_m^f = \tilde{P}_f, \tilde{P}_m^d = \tilde{P}_d, \; \forall m$. In such a case, there is no need to find N_m numerically since distinguishing sensing durations and detection thresholds of each SU is unnecessary. Therefore, Q_m^f (Q_m^d) directly becomes a function of the number of active SUs and $\tilde{P}^f$ ($\tilde{P}_m^d$) whose optimal value is defined as $\hat{P}_f^\star = \{\tilde{P}_f \mid Q_m^f = Q_{th}^f\}$ ($\hat{P}_d^\star = \{\tilde{P}_d \mid Q_m^d = Q_{th}^d\}$). Hence, required local false alarm, $P_m^{f^\star}$, and detection probabilities, $P_m^{d^\star}$, can be expressed as

$$\hat{P}_m^f = b_m^c \left(1 - P_m^{f^\star}\right) + \left(1 - b_m^c\right) P_m^{f^\star} \tag{31}$$

$$\hat{P}_m^d = b_m^c \left(1 - P_m^{d^\star}\right) + \left(1 - b_m^c\right) P_m^{d^\star} \tag{32}$$

which yields $\tilde{P}_m^{f^\star} = \frac{\hat{P}_m^{f^\star} - b_m^c}{1 - b_m^c}$ and $\tilde{P}_m^{d^\star} = \frac{\hat{P}_m^{d^\star} - b_m^c}{1 - b_m^c}$ by assuming $b_m^c < 0.5, \forall m$. Finally, substituting $\tilde{P}_m^{f^\star}$ and $\tilde{P}_m^{d^\star}$ into the right hand side of (2) and (3), and then solving (2) and (3) for N_m and ε_m, the optimal number of samples is determined as

$$N_m = \left[\frac{\mathcal{Q}^{-1}\left(P_m^{d^\star}\right)\sqrt{2\gamma_m + 1} - \mathcal{Q}^{-1}\left(P_m^{f^\star}\right)}{\gamma_m} \right]^2 \tag{33}$$

Accordingly, the procedure to find the set of SUs to be active is given in Algorithm 2 where SUs are only aware of their own battery level and SNR of cluster members. In line 1, SUs find vector of the feasible permutations $\boldsymbol{I_m}$ in which the required energy is not larger than the battery level, B_m^t, which is then reported to the FC. It is worth reminding that energy consumption of SU m changes with different set of active SUs, and $\boldsymbol{I_m}$ is the set of active SU permutations which is feasible with respect to battery level of SU m. Among reported permutations, the FC determines feasibility by checking if a permutation is reported by all SUs which are set to be active in that permutation. Afterwards, the FC calculates the achievable total throughput for $\boldsymbol{I}$ in line 4 and selects the ID with the maximum throughput, $I^\star$, which is then reported to SUs.

Algorithm 2 Myopic Activation Procedure (MAP)

Input: $\boldsymbol{E}$, $\mathcal{M}^\star$, B_m^t, γ_m, b_m^c, $\forall m$
Output: Set of SUs to be active.
1: $\boldsymbol{I_m} \leftarrow \underset{j}{\text{find}}$ s.t. $\boldsymbol{E}(m, j) \leq \boldsymbol{B_m^t}, \forall m$
2: SU m report $\boldsymbol{I_m}$'s to the FC, $\forall m$
3: $\boldsymbol{I} \leftarrow$ Determine feasible permutations among $\bigcup_m \boldsymbol{I_m}$.
4: $I^\star \leftarrow \underset{j \in \boldsymbol{I}}{\text{argmax}} \; R_t\left(\boldsymbol{I}(j)\right)$
5: **return** $I^\star$

VI. Numerical Results and Analysis

In order to gain a clear insight into the effect of sensing, reporting and energy harvesting features of SUs, SUs are assumed to have identical system parameters. Unless it is explicitly stated otherwise, we employ the parameter values summarized in Table II which draws mainly from [27]. Based on energy arrival rates averaged on a seasonal time scale, a typical solar panel is shown to have 15 mW/cm^2 power output [28]. Given the parameters in Table I and energy consumption model in equation (9), for example, 0.25 (0.75) seconds sensing (transmission) durations require around 260 mW power, which means a 16 cm^2 (i.e., 4 $cm \times 4$ cm) panel is sufficient for an SU. Considering the possible insufficiency of the RF energy harvesting rates and potential increase in solar panel efficiency, hybrid model provides a practical implementation for a more reliable energy source. Throughout the simulations, we employ the majority voting rule which has been shown as the most energy efficient. [15].

Par.	Value	Par.	Value	Par.	Value	Par.	Value
S	10	W	1 MHz	T_s	1 μs	T	1 s
P_m^s	110 mW	P_m^t	50 mW	P_m^c	210 mW	B_m	10 J
ξ_m	6 dB	ζ_m	0.35	Q_f^{th}	0.1	Q_d^{th}	0.9

Table II: Table of Parameters

A. Numerical Results for Asymptotic Analysis of EEH-CSS

To show the impact of SNR heterogeneity, we consider cooperation of 5 SUs with -5, -10, -15, -20, -25 SNRs in dB. Unless it is explicitly stated otherwise, we use the following parameter values throughout this subsection: $p = q = 0.8$, $b_m^c = 10^{-3}$, $\chi_m = 0.5\left(E_m^{c,0} + E_m^{c,1}\right)$, $\chi_m^{RF} = 0.1\left(E_m^{c,0} + E_m^{c,1}\right)$, $\forall m$. In Fig. 5, we compare α, P_m^d, $\bar{P}_m^d$, P_m^f, $\bar{P}_m^f$ of traditional (homogeneous) and proposed (heterogeneous) K-out of-N rules for EFS. On the other hand, Fig. 6 shows sensing durations and total achievable throughput corresponding to values in Fig. 5.

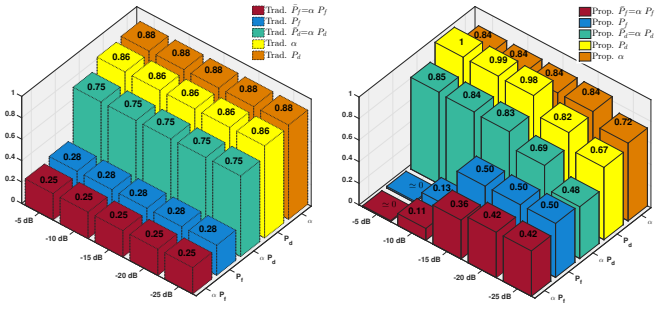

(a) Traditional (homogeneous) (b) Proposed (Heterogeneous)

Fig. 5: Comparison of α_m, P_m^d, $\bar{P}_m^d$, P_m^f, $\bar{P}_m^f$ for (a)traditional (homogeneous) and (b) proposed (heterogeneous) approaches for an EFS.

As explained in Section II-B, traditional K-out of-N rule treats SUs equivalently, which yields a Binomially distributed test statistic. For an EFS, optimal values of traditional approach can be seen in Fig. 5a where SUs have identical α_m, P_m^d, $\bar{P}_m^d$, P_m^f, and $\bar{P}_m^f$. Because the slowest SU with

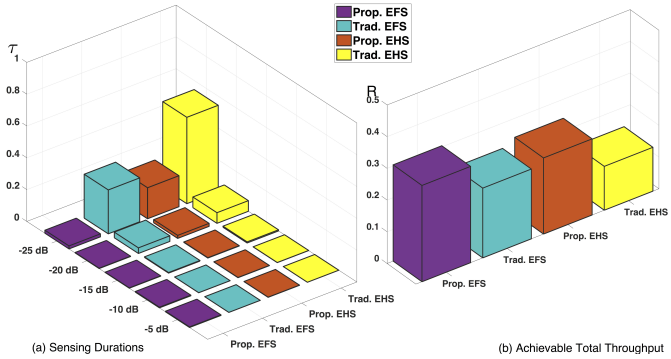

Fig. 6: Comparison of (a) τ_m and (b) $\bar{R}$ for EHS and EFS with traditional and proposed approaches.

the lowest SNR senses longer to achieve the performance of others, enforcing SUs with different sensing quality to have the same local detector performance increases the sensing energy cost and decreases $\bar{R}$ as shown in Fig. 6a and Fig. 6b, respectively. On the contrary, proposed K-out of-N rule allows SUs to have different local detection performance which yields a decrease in sensing energy cost and an increase in $\bar{R}$ as depicted in Fig. 6a and Fig. 6b, respectively. According to Fig. 5b, performance enhancement of the proposed approach is mostly because of that detection and false alarm probability of the slowest SU is relaxed to 0.5, which is compensated by requiring the SUs with high SNR to execute more accurate local detection. Therefore, this yields more balanced sensing duration and more time left for transmission since high SNR SUs compensate relaxation loss with an insignificant increase in sensing duration. Even though we do not present values of (α_m, P_m^d, $\bar{P}_m^d$, P_m^f, $\bar{P}_m^f$) for traditional and proposed approaches in EHSs due to space limitation, Fig. 6a and Fig. 6b clearly demonstrate the superiority of the proposed approach for EHSs, too. Furthermore, it is obvious from Fig. 6b that heterogeneous EFS gives the highest performance by mitigating the EHD constraint and taking the heterogeneity into consideration. It is worth mentioning that sensing costs depicted in Fig. 6 mainly determine the obtained results in Fig. 7-9 such that SUs with close sensing cost obtain performances close to each other.

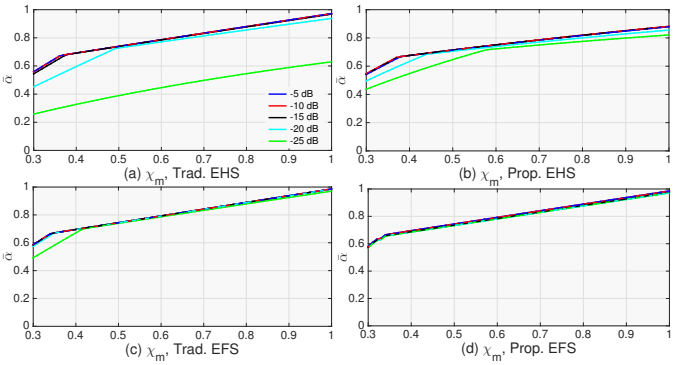

Fig. 7: $\bar{\alpha}_m$ vs. increasing energy arrival rates: (a) Traditional EHS, (b) Proposed EHS, (c) Traditional EFS, and (d) Proposed EFS.

The impact of composite energy arrival rate on probability

of sensing $\bar{\alpha}_m$ is illustrated in Fig. 7a-d where α_m intuitively increases with the energy arrival rate. In Fig. 7a, there is a significant difference between the slowest SU with -25 dB SNR and other SUs. Referring to Fig. 6a, decrease in the $\bar{\alpha}$ is mainly because of the high cost of sensing which increases the denominator of (27) and (28). Since the proposed approach generates a more balanced sensing cost as shown in Fig. 6a, taking the heterogeneity into account can close this gap as shown in Fig. 7b. Similar trends can be observed in Fig. 7c where the difference is not as significant as in Fig. 7c since EFS gains more benefit from energy arrivals than EHS. Finally, Fig. 7d shows $\bar{\alpha}$ of the EFS with proposed approach which achieves the most balanced performance as a result of Fig. 6a.

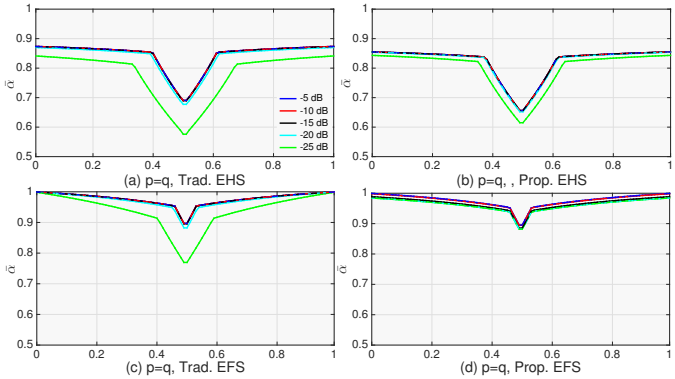

Fig. 8: $\bar{\alpha}_m$ vs. p and q: (a) Traditional EHS, (b) Proposed EHS, (c) Traditional EFS, and (d) Proposed EFS.

We demonstrate the impact of transition probabilities on $\bar{\alpha}_m$ in Fig. 8a-d where the common pattern is a result of the fact that $\bar{\alpha}_m^0$ and $\bar{\alpha}_m^1$ increase monotonically as $|1-p-q|$ increases since ℓ and monotonically decreases but υ monotonically increases. The reasoning behind this nature is hidden in the correlation constraints, that is, the higher value of $|1-p-q|$ gives more information to anticipate the next PC state more accurately given the current PC state. For example, $p=q=1$ ($p=q=0$) means that the PC state in the next slot will be the same as (opposite to) the current PC state. The difference in $\bar{\alpha}_m$ is due to the different sensing costs in traditional and proposed approaches in EHS and EFS as explained for Fig. 7. Again, Fig. 8d shows that $\bar{\alpha}$ of the EFS with proposed approach achieves the most balanced performance as a result of Fig. 6a.

Fig. 9a-d shows the impact of the BEP, b_m^c on $\bar{\alpha}_m$ where the common pattern is because of the fact that as the b_m^c increases, SUs are required to compensate the inaccuracy caused from reporting error by sensing longer. This results in more energy consumption, hence, less chance of being available for sensing. In Fig. 9a, the BEP wall occurs at 0.025 which is mostly driven by the slowest SU. The BEP wall of proposed EHS is observed between 0.4 and 0.5 since taking the heterogeneity into consideration mitigates the slowest SU effect in Fig. 9a. For the EFS in Fig. 9c, a better BEP wall is obtained compared to Fig. 9c since EFS is less vulnerable to the energy causality constraint. Finally, Fig. 9d shows that the EFS with proposed approach achieves the best performance in terms of $\bar{\alpha}_m$ and the BEP wall.

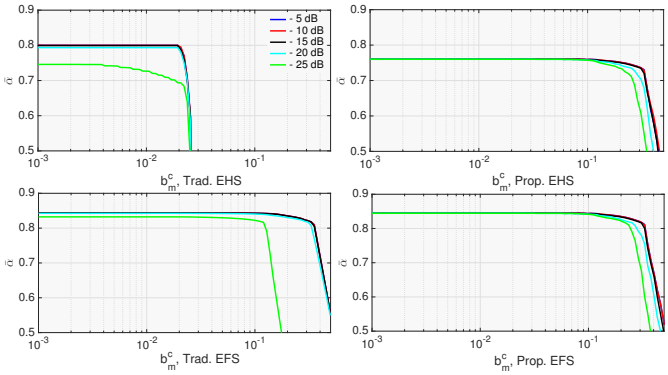

Fig. 9: $\bar{\alpha}_m$ vs. b_m^c: (a) Traditional EHS, (b) Proposed EHS, (c) Traditional EFS, and (d) Proposed EFS.

B. Performance Analysis of EH-SU Selection Heuristic

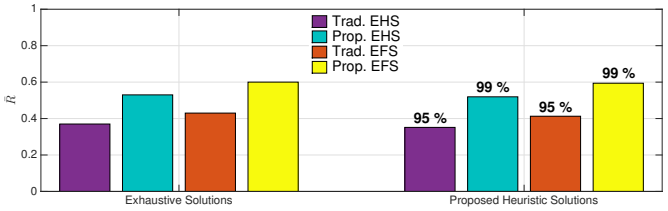

Fig. 10: Comparison of exhaustive and proposed heuristic solutions.

Fig. 10 compares the proposed heuristic solution presented in Algorithm 1 with the exhaustive solution where all possible combinations of EH-SU are calculated. Fig. 10 shows the average values of 30 different network scenarios where SUs have following randomized parameters: $\chi_m \in [0,1]$, $\gamma_m \in [-30,0]dB$, and $b_m^c \in [10^{-5},10^{-1}]$. As depicted in Fig. 10, heuristic solution achieves 95% and 99% of exhaustive performance using traditional and proposed approaches, respectively. We note that while the exhaustive solution takes $1-2$ hours on average, proposed heuristic generates results in less than a minute.

C. Performance Evaluation for MAP

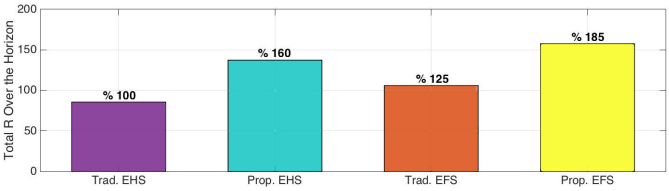

Fig. 11: Performance evaluation of MAP under different scenarios.

For performance evaluation of MAP, we consider an average of 100 different scenarios for 10 EH-SUs with random SNRs, $\gamma_m \in [-30,0]dB$, random energy arrival rates, $\chi_m \in [0,1]$, $\chi_m^{RF} \in [0,0.2]$, and random BEPs. $b_m^c \in [10^{-4},10^{-1}]$, $\forall m$. Fig. 11 shows the achieved total throughput of the SUs over 1000 time slots for different cases. The percentage over the bars shows the performance enhancement with respect to EHS with traditional CSS scheme. In EHS, exploiting the proposed

K-out of-N rule yields 60% more throughput which is a result of the more time left for more transmission and more chance to be active since the proposed method takes care of the sensing, reporting, and harvesting properties. As expected, the EFS with proposed heterogeneous CSS scheme introduces 20% more throughput by constantly harvesting the renewable energy in contrast to EHSs. Finally, EFS with the proposed K-out of-N rule gives the best performance with 85% more throughput since it combines the mitigation of EHD constraint and the proposed CSS schemes.

VII. Conclusions

In this paper, we have considered the design of a heterogeneous EEH-CSS scheme subject to fundamental EEH-CSS constraints. It was shown that taking the different harvesting, sensing, and reporting characteristics of EH-SUs into consideration can yield a better performance in terms of achievable throughput, energy consumption, and thus probability of being active. Since the active probability of an EH-SU is highly dependent on harvesting, sensing, and reporting attributes, we analyzed the asymptotic behavior of being active for a single EH-SU, which is then generalized to proposed heterogeneous EEH-CSS scheme. Given a potential set of SUs, determining the optimal subset of cooperating EH-SUs is of the essence to achieve maximum achievable total throughput. Since selection of this set inherently leads us to a combinatorial problem, which may be computationally infeasible even for small size of clusters, we proposed a fast yet high performance EH-SU selection heuristic exploiting the asymptotic cooperation behaviors. A myopic access procedure is then developed to jointly determine the active set of EH-SUs given the best subset of cooperating EH-SUs.

Appendix A
Proof of Theorem 1

We first note that this is a generalization of the proof in [5, Appendix C] where authors consider a deterministic amount of harvested energy, which is not suitable for the proposed hybrid model where the amount of harvested energy within a slot is stochastic. For their convenience, we refer readers to Fig. 4 for demonstration of the following discussion. The upper bound of α_m^0 can be found either on the borderline segment drawn between points $A = (1, \ell)$ and $B = \left(1, \min\left(1, \frac{\chi_m T - E_m^{c,0} + A_m}{E_m^{c,1} - B_m}\right)\right)$ or at the point of $\alpha_m^\ell = \left(\frac{\chi_m T}{E_m^{c,0} - A_m + \ell(E_m^{c,1} - B_m)}, \frac{\ell \chi_m T}{E_m^{c,0} - A_m + \ell(E_m^{c,1} - B_m)}\right)$. Thus, the upper bound of α_m^0 is obtained from $\overline{AB}$ and α_m^ℓ as $\alpha_m^0 \leq \min\left(1, \frac{X_m T}{E_m^{c,0} - A_m + \ell\left(E_m^{c,1} - B_m\right)}\right)$. On the other side, the lower bound of α_m^0 is obviously at the origin. Similarly, the upper bound of α_m^1 can be found either on the borderline segment drawn between points $C = (1/\upsilon, 1)$ and $D = \left(1, \min\left(1, \frac{\chi_m T - E_m^{c,1} + B_m}{E_m^{c,0} - A_m}\right)\right)$ or at the point of $\alpha_m^\upsilon = \left(\frac{\chi_m T}{E_m^{c,0} - A_m + \upsilon(E_m^{c,1} - B_m)}, \frac{\upsilon \chi_m T}{E_m^{c,0} - A_m + \upsilon(E_m^{c,1} - B_m)}\right)$. Hence, the upper bound of α_m^1 is obtained from $\overline{CD}$ and α_m^υ as $\alpha_m^1 \leq \min\left(1, \frac{\upsilon X_m T}{E_m^{c,0} - A_m + \upsilon\left(E_m^{c,1} - B_m\right)}\right)$. On the other hand, the lower bound of α_m^1 is at the origin. As a special case, feasible region reduces to a line for i.i.d. PC traffic model where $\alpha_m^0 = \alpha_m^1$ and $\ell = \upsilon = p + q = 1$. Accordingly, the upper bound of α_m^0 and α_m^1 is given by $\min\left(1, \frac{X_m T}{E_m^{c,0} + E_m^{c,1} - A_m - B_m}\right)$. The upper bounds of EFS can easily be found by substituting $A_m = 0$ and replacing B_m with C_m in above procedure.

Appendix B
Convexity Analysis of $\mathbf{P_1^l}$ and $\mathbf{P_1^u}$

Without loss of generality, we focus on the proof of convexity for $\log(\bar{R})$ which can then be adopted to the proof of convexity for $\log(R_t)$ by keeping α_m^0 and α_m^1 constant. The decoupled convexity (concavity) of $\log(Q_f)$ ($\log(Q_d)$) can be obtained by the log-concavity of Poisson-Binomial distribution as in [15], [16].

A. Convexity Analysis of Lower Level Problem, $\mathbf{P_1^l}$

$\searrow$	P_m^d	P_m^f	$\bar{P}_m^d$	$\bar{P}_m^f$	Q_d	Q_f	$\bar{Q}_d$	$\bar{Q}_f$	$\bar{R}$
ε_m	$\nearrow$	$\nearrow$	$\nearrow$	$\nearrow$	$\nearrow$	$\nearrow$	$\nearrow$	$\nearrow$	$\searrow$

$\nearrow$	P_m^d	P_m^f	$\bar{P}_m^d$	$\bar{P}_m^f$	Q_d	Q_f	$\bar{Q}_d$	$\bar{Q}_f$	$\bar{R}$
α_m^0	$\leftrightarrow$	$\leftrightarrow$	$\nearrow$	$\nearrow$	$\leftrightarrow$	$\leftrightarrow$	$\nearrow$	$\nearrow$	$\searrow$
α_m^1	$\leftrightarrow$	$\leftrightarrow$	$\nearrow$	$\nearrow$	$\leftrightarrow$	$\leftrightarrow$	$\nearrow$	$\nearrow$	$\searrow$

Table III: Observation on $\bar{Q}_f$, $\bar{Q}_d$, and $\bar{R}$ with respect to ε_m, α_m^0, and α_m^1.

To check the convexity of C3 and C4, we consider the following observation given in Table III. For fixed α_m^0, α_m^1, and a decreasing ε_m, $\bar{Q}_f$ is increasing and upper bounded by Q_f^{th}. Thus, once $\bar{Q}_f = Q_f^{th}$ is satisfied, we cannot decrease ε_m since it violates $\bar{Q}_f \leq Q_f^{th}$ and reduces $\bar{R}$. On the other hand, for a decreasing ε_m, $\bar{Q}_d$ is also increasing along with a decreasing objective, $\bar{R}$. Therefore, once $\bar{Q}_d = Q_d^{th}$ is attained, there is no need to decrease ε_m since it reduces $\bar{R}$. As a result, the optimal $\bar{R}$ is obtained when $\bar{Q}_f = Q_f^{th}$ and $\bar{Q}_d = Q_d^{th}$ is attained. As can be seen from Table III, the same observations hold for increasing α_m^0 (α_m^1) with fixed α_m^1 (α_m^0) and ε_m. Accordingly, we treat $\bar{Q}_f$ and $\bar{Q}_d$ in $\bar{\alpha_m^0}$ and $\bar{\alpha_m^1}$ as constant by setting $\bar{Q}_f = Q_f^{th}$ and $\bar{Q}_d = Q_d^{th}$. In this case, C3 and C4 reduces to a linear upper-lower bound range for α_m^0 and α_m^1, respectively. In the objective,

$$\log(\bar{R}) = \log(\pi_0) + \log\left(1 - \bar{Q}_f\right) + \log\left(\sum_m R_m\right), \quad (34)$$

the first term and second term is constant with respect to $(\alpha_m^0, \alpha_m^1, \varepsilon_m)$. For the middle term, we exploit the above observation and set $\bar{Q}_f = Q_f^{th}$ which is also constant. Accordingly, $\mathbf{P_1^u}$ is reduced to a convex feasibility problem.

B. Convexity Analysis of Upper Level Problem, $\mathbf{P_1^u}$

In the objective given in (34), the first term is a constant and the second term is concave due the log-concavity of Poisson-Binomial distribution. For the last term, we consider each summand separately as $R_m = g(Y, Z) = \frac{Y}{T} \log\left(1 + \frac{Z}{Y}\right)$ where $Z = E_m$ and $Y = T - \Gamma = T - \max_m(N_m T_s)$. $g(Y, Z)$ is monotonically increasing over (Y, Z) since $Y,\ Z \geq 0$ and the

first derivative of $g(Y,Z)$ is $\frac{\partial g(Y,Z)}{\partial Y} = \log\left(1+\frac{Z}{Y}\right) - \frac{Z}{Y+Z} > 0$ due to the property of logarithm function: $\log(1+x) > x/(1+x)$ for $x > 0$. Moreover, $g(Y,Z)$ is jointly concave on (Y,Z) since it is a perspective function of $\log(1+Z)$, which is concave for $Z \geq 0$, and the perspective operation preserves the convexity [29]. $\Gamma = \max_m (N_m T_s)$ is a piecewise maximum of functions $f_m = N_m T_s$ which is linear over N_m and constant for N_n, $\forall n \neq m$. Since the piecewise maximization preserves the convexity and f_m is linear, $Y = T - \Gamma$ is a concave function of N_m which is followed from the convex composition rules and negative sign of Γ. Since the last term is log-sum of the concave R_ms, it is also a concave function of N_m which is again follows from the convex composition rules.

REFERENCES

[1] J. Andrews *et al.*, "What will 5g be?" *IEEE J. Sel. Areas Commun.*, vol. 32, no. 6, pp. 1065 –1082, July 2014.

[2] S. Pollin *et al.*, "Meera: Cross-layer methodology for energy efficient resource allocation in wireless networks," *IEEE Trans. Wireless Commun.*, vol. 7, no. 1, pp. 98–109, 2008.

[3] M. Webb *et al.*, "Smart 2020: Enabling the low carbon economy in the information age," *The Climate Group. London*, vol. 1, no. 1, pp. 1–1, 2008.

[4] O. Ozel *et al.*, "Fundamental limits of energy harvesting communications," *IEEE Commun. Mag.*, vol. 53, no. 4, pp. 126–132, 2015.

[5] S. Park and D. Hong, "Achievable throughput of energy harvesting cognitive radio networks," *IEEE Trans. Wireless Commun.*, vol. 13, no. 2, pp. 1010–1022, 2014.

[6] A. Sultan, "Sensing and transmit energy optimization for an energy harvesting cognitive radio," *IEEE Wireless Commun. Lett.*, vol. 1, no. 5, pp. 500–503, 2012.

[7] S. Park *et al.*, "Cognitive radio networks with energy harvesting," *IEEE Trans. Wireless Commun.*, vol. 12, no. 3, pp. 1386–1397, 2013.

[8] S. Park and D. Hong, "Optimal spectrum access for energy harvesting cognitive radio networks," *IEEE Trans. Wireless Commun.*, vol. 12, no. 12, pp. 6166–6179, 2013.

[9] S. Yin *et al.*, "Achievable throughput optimization in energy harvesting cognitive radio systems," *IEEE J. Sel. Areas Commun.*, vol. 33, no. 3, pp. 407–422, Mar. 2015.

[10] H. Liu *et al.*, "Optimal cooperative spectrum sensing strategy in cognitive radio networks exploiting rf-energy harvesting," in *proc. IEEE WCSP*, 2015, pp. 1–5.

[11] K. Li *et al.*, "Energy-harvesting cognitive radio systems cooperating for spectrum sensing and utilization," in *proc. IEEE GLOBECOM*, 2015.

[12] P. Pratibha, K. H. Li, and K. C. Teh, "Dynamic cooperative sensing-access policy for energy-harvesting cognitive radio systems," *IEEE Trans.Veh. Technol.*, 2015.

[13] S. Luo *et al.*, "Optimal save-then-transmit protocol for energy harvesting wireless transmitters," *IEEE Trans. Wireless Commun.*, vol. 12, no. 3, pp. 1196–1207, Mar. 2013.

[14] A. Celik, A. Alsharoa, and A. Kamal, "Hybrid energy harvesting cooperative spectrum sensing in heterogeneous crns," in *proc. IEEE GLOBECOM Workshops*, Dec. 2016.

[15] A. Celik and A. E. Kamal, "Multi-objective clustering optimization for multi-channel cooperative spectrum sensing in heterogeneous green crns," *IEEE Trans. Cogn. Commun. Netw.*, vol. 2, no. 2, pp. 150–161, June 2016.

[16] ——, "Green cooperative spectrum sensing and scheduling in heterogeneous cognitive radio networks," *IEEE Trans. Cogn. Commun. Netw.*, vol. 2, no. 3, pp. 238–248, Sept 2016.

[17] E. Axell *et al.*, "Spectrum sensing for cognitive radio: State-of-the-art and recent advances," *IEEE Signal Processing Mag.*, vol. 29, no. 3, pp. 101–116, May 2012.

[18] E. C. Y. Peh *et al.*, "Optimization of cooperative sensing in cognitive radio networks: A sensing-throughput tradeoff view," *IEEE Trans. Veh. Technol.*, vol. 58, no. 9, pp. 5294–5299, Nov. 2009.

[19] A. Celik and A. E. Kamal, "More spectrum for less energy: Green cooperative sensing scheduling in crns," in *proc. IEEE ICC*, 2015.

[20] M. Fernandez and S. Williams, "Closed-form expression for the Poisson-binomial probability density function," *IEEE Trans. Aerosp. Electron. Syst.*, vol. 46, no. 2, pp. 803–817, Apr. 2010.

[21] R. Zhang and C. K. Ho, "Mimo broadcasting for simultaneous wireless information and power transfer," *IEEE Trans. Wireless Commun.*, vol. 12, no. 5, pp. 1989–2001, May 2013.

[22] B. Medepally and N. B. Mehta, "Voluntary energy harvesting relays and selection in cooperative wireless networks," *IEEE Trans. Wireless Commun.*, vol. 9, no. 11, pp. 3543–3553, November 2010.

[23] S. Cui, A. J. Goldsmith, and A. Bahai, "Energy-constrained modulation optimization," *IEEE Trans. Wireless Commun.*, vol. 4, no. 5, pp. 2349–2360, 2005.

[24] S. Chaudhari *et al.*, "Bep walls for cooperative sensing in cognitive radios using k-out-of-n fusion rules," *Signal Processing*, vol. 93, no. 7, pp. 1900–1908, 2013.

[25] Q. Zhao *et al.*, "On myopic sensing for multi-channel opportunistic access: structure, optimality, and performance," *IEEE Trans. Wireless Commun.*, vol. 7, no. 12, pp. 5431–5440, 2008.

[26] S. H. A. Ahmad, M. Liu, T. Javidi, Q. Zhao, and B. Krishnamachari, "Optimality of myopic sensing in multichannel opportunistic access," *IEEE Trans. Inf. Theory*, vol. 55, no. 9, pp. 4040–4050, 2009.

[27] Y. Pei *et al.*, "Energy-efficient design of sequential channel sensing in cognitive radio networks: optimal sensing strategy, power allocation, and sensing order," *IEEE J. Sel. Areas Commun.*, vol. 29, no. 8, pp. 1648–1659, 2011.

[28] Y. Mao, Y. Luo, J. Zhang, and K. B. Letaief, "Energy harvesting small cell networks: feasibility, deployment, and operation," *IEEE Communications Magazine*, vol. 53, no. 6, pp. 94–101, June 2015.

[29] S. Boyd and L. Vandenberghe, *Convex optimization*. Cambridge university press, 2004.